Laboratory spectroscopy of meteorite samples at UV-Vis-NIR wavelengths: Analysis and discrimination by principal components analysis

Antti Penttilä[a,*], Julia Martikainen[a], Maria Gritsevich[a], Karri Muinonen[a,b]

[a] *Department of Physics, P.O. Box 64, FI-00014 University of Helsinki, Finland*
[b] *Finnish Geospatial Research Institute FGI, National Land Survey of Finland, Geodeetinrinne 2, FI-02430 Masala, Finland*

Abstract

Meteorite samples are measured with the University of Helsinki integrating-sphere UV-Vis-NIR spectrometer. The resulting spectra of 30 meteorites are compared with selected spectra from the NASA Planetary Data System meteorite spectra database. The spectral measurements are transformed with the principal component analysis, and it is shown that different meteorite types can be distinguished from the transformed data. The motivation is to improve the link between asteroid spectral observations and meteorite spectral measurements.

Keywords: Meteorites, spectroscopy, principal component analysis

1. Introduction

While a planet orbits the Sun, it is subject to impacts by objects ranging from tiny dust particles to much larger asteroids and comet nuclei. Such collisions of small Solar System bodies with planets have taken place frequently over geological time and played an important role in the evolution of planets and development of life on the Earth. Every day approximately 30–180 tons of interplanetary material enter the Earth's atmosphere [1, 2]. This material is mostly represented by smaller meteoroids that undergo rapid ablation in the atmosphere. Under favorable initial conditions part of a meteoroid may survive the atmospheric entry and reach the ground [3]. The fragments recovered on the ground are called meteorites, our valuable samples of the Solar System.

Most meteoroids originate in comets or come from the asteroid belt, having been perturbed by the gravitational influences of planets [4]. Some meteoroids are collision impact debris ejected from bodies such as Mars or the Moon [5]. Furthermore, some fragments are remnants of parent bodies which do not longer exist in the Solar System. Their diameters range from a few meters to hundreds of kilometers and they are primitive meaning that they

*Corresponding author
Email address: antti.i.penttila@helsinki.fi (Antti Penttilä)

never reached high enough densities to differentiate and form a crust, mantle, and core. A notable exception to this is (4) Vesta which is currently the only known intact differentiated asteroid.

A meteorite-to-be starts its journey to the Earth after an impact: another object impacts the surface of the parent asteroid fragmenting it and removing pieces from its surface, and in some cases even from its core or mantle. The impact causes shock pressure on the released piece which can change its structure and composition thus affecting other properties, such as spectral features. The meteoroid's journey to the Earth is long and during it the space weathering process alters its surface. At some point the fragment likely enters an orbit that is in resonance with Mars or Jupiter making the orbit unstable. The fragment is pushed towards the Earth's orbit and eventually it enters the atmosphere, finally hitting the ground where its surface is further altered by oxidation caused by terrestrial weathering.

Asteroids have remained almost the same for 4.5 billion years. There are three ways to study them: sample-return, rendezvous, or flyby space missions, ground-based observations at different wavelengths, and the meteorite study. Sample-return, rendezvous, and flyby space missions are expensive and quite rare, and ground-based observations have a low resolution because asteroids are small and distant objects. Meteorites are almost undisturbed samples of their parent bodies, so studying them provides us information on their parent asteroid's composition and structure and expands our knowledge of the evolution of the small bodies in the early Solar System.

1.1. Meteorite classification

Meteorite classification is based on mineralogical and petrographic characteristics. The current classification scheme divides meteorites into chondrites, primitive chondrites and achondrites [6].

Chondrites are the most common meteorite type that fall to the Earth. They are rocky meteorites that have not melted or differentiated, and they often contain small components, such as chondrules, Ca-Al-rich inclusions (CAIs) and amoeboid olivine aggregates (AOAs), which have been born independently in the protoplanetary disk by high-temperature evaporation and condensation processes [6]. In other words, chondrites have preserved physical and chemical properties of the protoplanetary disk. Chondrites can be further divided into ordinary chondrites (that can be divided into H, L, and LL chondrites), carbonaceous chondrites and enstatite chondrites.

Achondrites do not contain chondrules, CAIs, or AOAs. They are meteorites that have been at least partially melted and their parent bodies have been differentiated. Primitive achondrites cannot be classified into chondrites or achondrites: there is some melting in them but, chemically, they resemble chondrites [6].

Based on petrographic characteristics and the degree of shock pressure and terrestrial weathering the meteorites have experienced, they can be further classified. The petrologic grade describes how the minerals are mixed and distributed and how much thermal metamorphism the meteorite has experienced (apart from achondrites, which do not have a petrologic grading system, because they have undergone some melting). As soon as the meteoroid reaches the atmosphere, the Earth's environment begins to alter its surface. Terrestrial

weathering, which includes both chemical weathering and physical weathering, affects the meteorite's chemistry, mineralogy, structure and composition [7]. The longer the meteorite is exposed to the weathering effects on the ground the more it is altered. That is why "falls", meteorites that are collected after their fall from the space was observed, are more valuable samples than all the other "finds" because they have not had time to be substantially altered by terrestrial weathering. It has also been noticed that finds collected from Antarctica are less weathered than other finds. This suggests that the environment plays a big role on how much a meteorite is altered due to weathering.

The grade of the shock describes how much shock a meteorite has experienced during its space history. Lightly shocked meteorites contain dark melt veins: the impact that releases the fragment from its parent body initiates shock metamorphism and created veins and pockets are filled with shock-melted material such as iron metal and sulfides [8, 9]. Strongly shocked meteorites exhibit more pronounced shock-wave related melting and deformation, which occurs as fracturing, twinning, and mosaicism within the minerals [10].

1.2. Spectroscopy

Asteroid spectroscopy began in the late 1960s when sensitive photoelectric detectors were used to obtain high precision measurements of the Solar System bodies in the wavelength range of 0.32–1.1 µm. The pioneer of this field, Tom McCord, did the first spectroscopic observations of the Moon in 1968, and after that successfully observed asteroid (4) Vesta. At that time crystal field theory, which explains physical principles for absorptions caused by transition metal ions in mineral structures, was further developed. In the early 1970s, Clark R. Chapman led an asteroid survey that resulted in many papers describing asteroid spectra in the 0.3–1.1 µm range. Chapman and Salisbury[11] compared data on asteroid and meteorite properties proving this field of study to be worth pursuing. In the mid-1970s, Michael J. Gaffey performed a detailed laboratory study of the meteorite spectral properties in the wavelength range of 0.35–2.5 µm resulting in a paper[12] that overviewed the spectral properties of meteorites in that specific wavelength range.

A spectrum of an object describes how much electromagnetic radiation is scattered or absorbed by the object at different wavelengths. Spectra have different shapes: there are slopes and peaks, broad troughs and narrow troughs, each feature telling a story of the mineralogy and petrology of the object. In the asteroid and meteorite spectral studies, visible and near-infrared reflectance spectra are used to determine the mineralogy and petrology of the object [12]. Slopes tell us how much light the object reflects depending on the wavelength: red slope means that more light is reflected at longer wavelengths, respectively blue slope indicates that less light is reflected at longer wavelengths. The slopes are used in classification, because they tell about the composition, particle size, and space-weathering state of the object. The troughs in the spectra are called absorption bands, and they are usually formed when transition-metal silicates (Sc, Ti, V, Cr, Mn, Fe, Co, Ni, Cu) absorb light [13]. Meteorites and asteroids consist of different minerals, olivine and pyroxene being the most abundant ones. These minerals have their own dominant spectral features in the visible and near-infrared regions. Olivine has a broad asymmetric absorption feature centered near 1.0 µm, while pyroxene has two narrow symmetric absorption features centered

near 0.9 and 2.0 µm [14]. Combinations of the minerals change the strength of the absorption bands and move the locations of their minima. Also carbon and metal change the spectral features. Carbon, which is also common in some meteorites, darkens the spectra, whereas nano-phase iron increases the slope of the spectra toward longer wavelengths [15].

Spectra is usually normalized, i.e., divided by the reflectance at some fixed wavelength, often 550 nm, if that is available in the data. The normalization enables the comparison of the spectral absorption bands and the slopes without the effect of the average albedo of the target. In spectral observations of distant targets, the absolute size of the point-like target can be unknown, and thus the absolute albedo remains also unknown. In laboratory spectroscopy, the absolute reflectance level can be resolved by comparing the measured reflectance into measurements of an (almost) ideal Lambertian surface such as Spectralon. However, even when comparing laboratory spectra, normalization might be needed. There can be a general absorbing agent present in the matrix of our target material resulting in different average albedo between samples. Let us say that we are comparing two samples with the same mineral of interest, described here with its spectral absorption coefficients $\kappa := \kappa(\lambda)$, where λ is the wavelength. With an absorbing agent mixed in the matrix, the effective absorption coefficient becomes $\kappa + \kappa_x$, where κ_x presents the unknown absorbing material.

The reflectance spectrum is governed by the amount of transmission t in the material, which can be approximated by the Beer-Lambert law by $t = \exp(-4\pi d\kappa)$, where d is the distance traveled in the matrix. Now, if the transmissions by a target with an unknown but spectrally constant absorbing agent is normalized at some wavelength where $\kappa(\lambda_0) = \kappa_0$, it becomes

$$t = \frac{\exp\left(-4\pi d\left(\kappa + \kappa_x\right)\right)}{\exp\left(-4\pi d\left(\kappa_0 + \kappa_x\right)\right)} = \exp\left(-4\pi d\left(\kappa - \kappa_0\right)\right), \tag{1}$$

and the unknown absorbing agent κ_x is eliminated. The normalization also helps when comparing spectra from particulate samples with different grain sizes, but it should be noted that with smaller grain sizes there will be more reflections from surfaces. Thus, the distance d traveled by the light will be smaller. Looking at Eq. (1) we see that the different distances will not be eliminated, therefore the spectra will not be identical after the normalization. However, the wavelengths of the absorption bands are not varying, only the depths.

The article is organized so that in Sec. 2 we introduce the studied meteorite samples, our spectrometric laboratory, and the principal component analysis method. In Sec. 3 we present the spectral measurements of meteorites, followed by their analysis. The preliminary results from the analysis described here were presented in the Master's thesis by J. Martikainen [16].

2. Materials and methods

2.1. Meteorite samples

The reflectance spectra of 30 meteorite samples were measured (see Table 1). The samples were borrowed from Geological Museum of the Finnish Museum of Natural History. Each sample was chosen so that it was a meteorite fall, collected shortly after its passage

through the atmosphere was observed. All the samples had a characteristic size of a few centimeters, at least. The measured surfaces were either polished or unpolished and contained no fusion crust. Among the measured meteorite samples 23 were ordinary chondrites, 4 were HED meteorites, one was an aubrite, one was a carbonaceous chondrite, and one was an enstatite. Images of the meteorites are shown in Figs. 1–3.

Table 1: The measured meteorite samples.

Meteorite	Type	Meteorite	Type
Abee	E4	Kisvarsany	L6
Agen	H5	Menow	H4
Allende	CV	Nammianthal	H5
Ausson	L5	Norton County	Aubrite
Buschnof	L6	Nyirabrany	LL5
Cape Girardeau	H6	Pacula	L6
Castalia	H5	Sevrukovo	L5
Chitado	H6	Sioux County	Eucrite
Collescipoli	H5	Souslovo	L4
Dhurmsala	LL6	St. Germain-du-Pinel	H6
Durala	L6	St. Michel	L6
Ergheo	L5	Stannern	Eucrite
Jilin	H5	Ställdalen	H5
Johnstown	Diogenite	Tieschitz	H/L3.6
Juvinas	Eucrite	Vernon County	H6

For comparison, we supplemented our meteorite samples with the measured spectra from the NASA Planetary Data System (PDS) meteorite spectra database [17]. From that data collection, we included spectral measurements of 14 meteorite samples. The chosen meteorite samples were all whole rock samples, not small particles, and they did not contain any fusion crust. These samples are listed in Table 2.

Table 2: Chosen meteorite samples in the PDS meteorite spectra database.

Meteorite	Type	Meteorite	Type
Aumale	L6	Paragould	LL5
Bald Mountain	L4	Rose City	H5
Buschnof	L6	Soko-Banja	LL4
Cynthiana	L4	St. Michel	L6
Johnstown	Diogenite	Stannern	Eucrite
Knyahina	L5	Tatahouine	Diogenite
Murchison	CM2	Warrenton	CO3

Figure 1: Images of the measured H chondrites.

Figure 2: Images of the measured L and LL chondrites.

Figure 3: Images of the measured enstatite chondrite (Abee), aubrite (Norton County), carbonaceous chondrite (Allende), and HEDs.

2.2. Laboratory spectrometer

The reflectance spectra of our meteorite samples were measured with the University of Helsinki integrating-sphere UV-Vis-NIR spectrometer. This spectrometer is a modular Gooch & Housego OL 750 automated spectroradiometer (see Fig. 4). It contains a light source module with a 150 W quartz tungsten-halogen source for the Vis-NIR range (up to 3.2 µm), and recently also a 40 W deuterium arc source for the UV range (from 0.25 µm).

The monochromator module has blazing gratings operating through the wavelength range of 0.25–3.2 µm. The monochromatic light is also collimated and shaped with slits and/or circular apertures. The measurements discussed here were carried out using either a 2.5 mm slit and a 2.5 mm aperture or a 5.0 mm slit and a 5.0 mm aperture depending on the size of the meteorite piece. The size of the beam spot on the sample is approximately two times the size of the latter aperture/slit.

The monochromatic and collimated light is guided into an integrating sphere, either coated with polytetrafluoroethylene (PTFE, for wavelengths up to 2.5 µm) or with gold (up to 3.2 µm). The light beam can be guided either into the sphere wall or into the sample that is located in the bottom of the sphere. The direct specular reflection is forwarded into a beam trap. The sample holder in the bottom of the sphere is made of dark and spectrally featureless black teflon.

Finally, the reflected light that is diffusely scattered in the sphere is measured with our three detectors. We apply a cooled photomultiplier tube detector for wavelengths 0.25–0.42 µm, silicon detector for 0.4–1.1 µm, and a PbS detector for 1.05–3.2 µm. The overlapping wavelengths are used to check that the change from one detector to another does not produce discontinuities in the results.

With all the detectors the measurement is always related both to a reflectance standard measurement with the current configuration and a known calibration values of that standard. The final reflectance value R is given by

$$R(\lambda) = \frac{F_4(\lambda, C)}{F_3(\lambda, C)} \frac{F_2(\lambda, C)}{F_1(\lambda, C)} R_s(\lambda), \tag{2}$$

where F's are the absolute measured reflectance, R_s the known calibration reflectance of the standard, λ the wavelength, and C the current configuration (i.e., light source, slits, integrating sphere, detector integration time) of the measurement. The different measurements F are such that F_1 is with the beam off from the sample and with the reflectance standard as the sample; F_2 is with the reflectance standard and the beam on the sample; F_3 is with the actual sample in-place and the beam off the sample; F_4 is with the actual sample and the beam on the sample. The measurements F_1 and F_2 are calibration measurements that are done from time to time to adopt to changes in, e.g., light source power and detector efficiency, while F_3 and F_4 are the actual measurements. The calibration standard, for which we have the factory-provided known reflectance, is either a PTFE or a slightly rough gold plate.

During the time the meteorite measurements discussed here were done, the UV light source and the gold-coated integrating sphere were not installed. Therefore, the wavelengths reported here are limited to a range of 0.3 to 2.5 µm.

Figure 4: The University of Helsinki UV-Vis-NIR spectrometer.

2.3. Principal Component Analysis

Principal component analysis (PCA) is used to analyze the reflectance spectra of the meteorite samples. PCA is a statistical tool for analyzing large data sets with correlated variables, such as the wavelengths in the spectrum. It can be used to identify patterns in multidimensional data and thus classify spectra. PCA removes the correlations between different variables of the data set and transforms the data to a new coordinate system by using an orthogonal transformation so that the new coordinates have the largest variances. By leaving out the coordinates which have the smallest variances, the number of dimensions can be reduced. The new coordinates are called principal components that represent the data set and help to group the observations.

For the PCA, the data must be in a data matrix where each row represents one reflectance spectrum measurement of a certain meteorite piece and each column represents a reflectance value of a specific wavelength. The columns of the data matrix are called variable vectors.

The data must be mean-centered so that the mean value for each variable vector is zero. By subtracting an average matrix from the data matrix the mean-centered data matrix ($\mathbf{X}$) can be acquired:

$$\mathbf{X} = \mathbf{M} - \mathbf{1}\boldsymbol{\mu}^T, \tag{3}$$

where $\boldsymbol{\mu}$ is the average vector, $\mathbf{1}$ is a vector of ones, and $\mathbf{M}$ is the data matrix. The next step is to calculate a covariance or correlation matrix from the mean-centered data. Because the spectral data is of the same scale and unit, the covariance matrix is used. The covariance matrix of $\mathbf{X}$ is:

$$\boldsymbol{\Sigma} = \frac{1}{N-1}\mathbf{X}^T\mathbf{X}. \tag{4}$$

The eigenvalue decomposition $\boldsymbol{\Sigma} = \mathbf{V}\boldsymbol{\Lambda}\mathbf{V}^T$ of the covariance matrix gives us the PCA coordinate basis as the columns of the eigenvector matrix $\mathbf{V}$, and the eigenvalues in the diagonal matrix $\boldsymbol{\Lambda}$. The data $\mathbf{X}$ projected into the PCA space is given by

$$\mathbf{Z} = \mathbf{X}\mathbf{V}. \tag{5}$$

The total variance of the original data is re-arranged in the PCA, and the eigenvalues $\mathbf{\Lambda}_{i,i}$ give the re-arranged variances for the columns (i.e., variables) i in $\mathbf{Z}$. If the variables in the original data are highly correlated, the re-arranged total variance is concentrated on the first few eigenvalues/vectors, meaning that the dimension of the variables can be reduced by taking only the first few columns of $\mathbf{Z}$ into further analysis.

With our application of meteorite spectra, we perform the PCA analysis here on the normalized spectra. This removes the significance of the average albedo on the results.

3. Results and Discussion

3.1. Spectral measurements

The measurement campaign resulted in 30 spectra of our meteorite samples. The H, L, and LL chondrites, see Figs. 5–7, have similar spectral features — a broad maximum in the spectrum at 0.7 µm, and an absorption feature near 0.9 µm. The reflectivity rises toward 1.5 µm, and a broad absorption band is centered at 1.9 µm. These characteristic spectral features are caused by olivine and pyroxene, the most abundant minerals in ordinary chondrites. There is also a small bump in the spectrum resulting from an absorption feature around 1.3 µm caused by feldspar, or by Fe^{2+} in M1 site in olivine or pyroxene[18, 19].

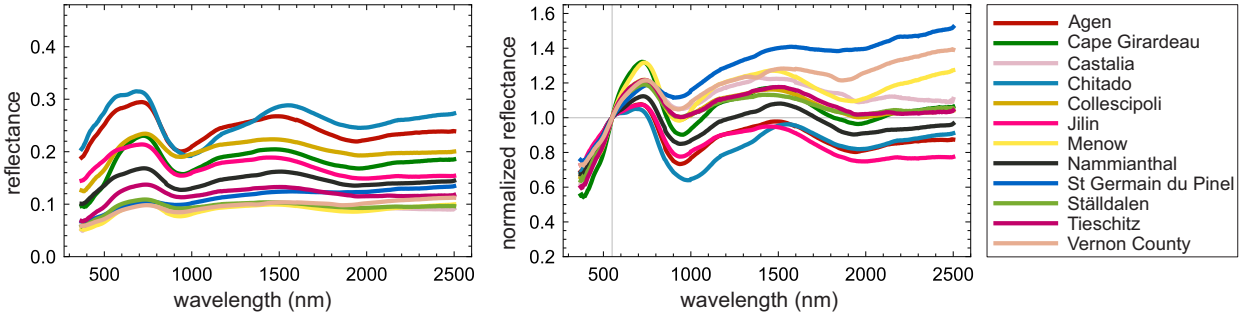

Figure 5: The measured reflectance spectra of H chondrites. In the left, the reflectance values without normalization, and in the right, the normalized (at 0.55 µm) reflectance values.

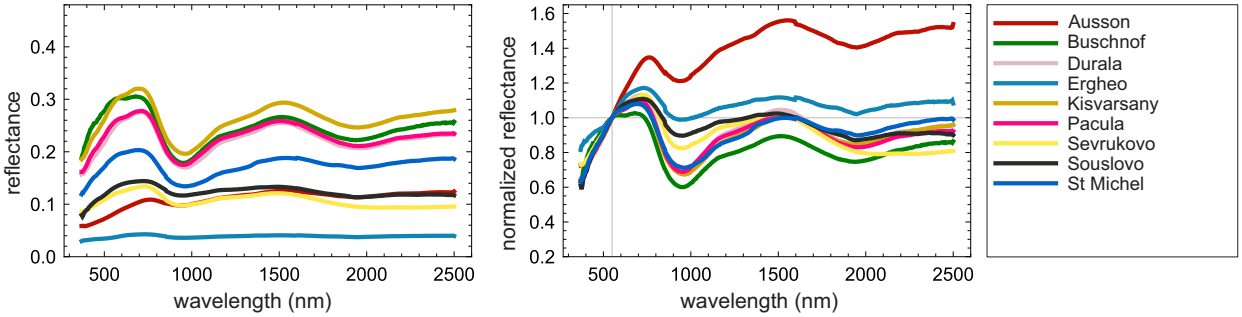

Figure 6: As in Fig. 5 for the measured reflectance spectra of L chondrites.

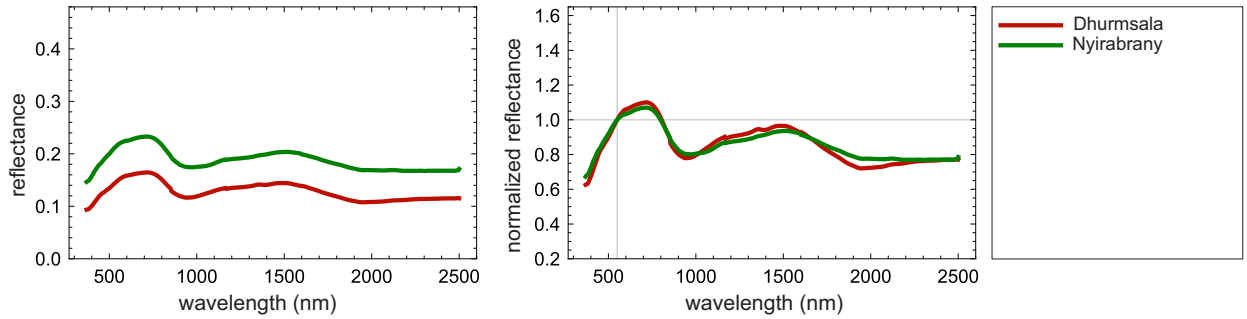

Figure 7: As in Fig. 5 for the measured reflectance spectra of LL chondrites.

The HED (howardite, eucrite, diogenite) meteorites, originating from (4) Vesta, do not contain olivine, so their spectra are dominated by pyroxene, see Fig. 8. The spectrum rises deeply in the blue, has a deep absorption band centered at 0.9 µm, a maximum in reflectance at about 1.5 µm, and a broad absorption feature centered at 2.0 µm. Eucrites also contain feldspar, causing a small feature at 1.3 µm (together with the Fe^{2+} in M1 in pyroxene), which is absent or weak in the reflectance spectra of howardites and diogenites.

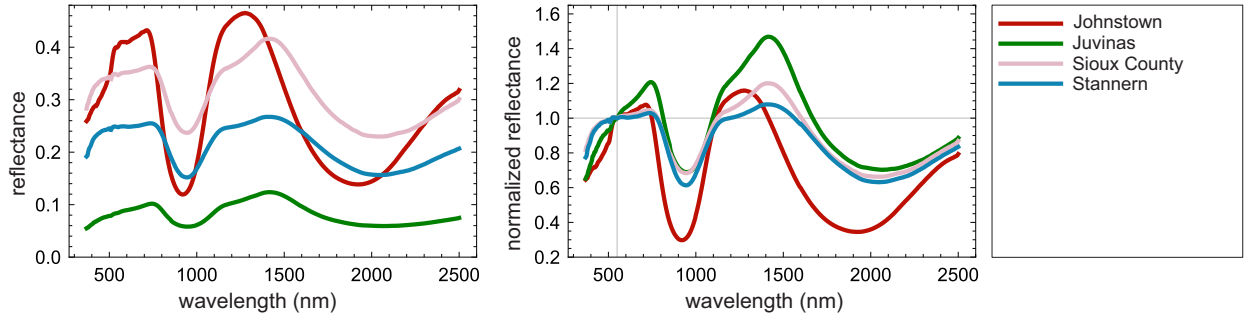

Figure 8: As in Fig. 5 for the measured reflectance spectra of HED meteorites.

The spectrum of the Norton County meteorite is typical for an aubrite, see Fig. 9. The reflectance is reddened in the visible region and decreases slightly toward longer wavelengths. Enstatite chondrites consist of pure enstatite and metal. Their spectrum is typically featureless with a red slope in the visible and a slowly increasing reflectance in the infrared. The spectrum of Abee shows decreasing in the reflectance before it increases slightly. The reflectance spectra of Allende has a reddened curve in the visible and a slightly increasing infrared reflectance. The overall albedo of the reflectance spectra for both Abee and Allende is low.

3.2. Principal component analysis

The purpose of the PCA is to identify if we can extract features from the spectra that can group similar targets together. If we achieve this, we can claim to have deduced quantitatively the distinctive features in the spectral taxonomy. As we complement our data of 30 spectral measurements with the 14 spectra from the PDS meteorite spectra database and

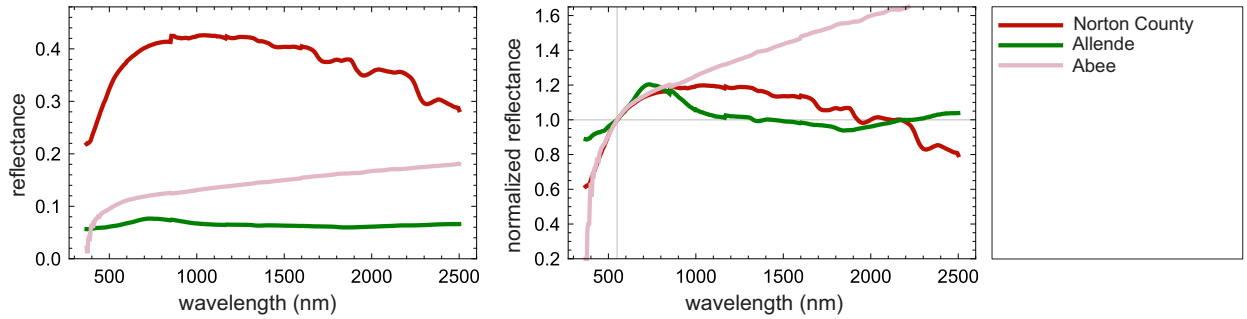

Figure 9: As in Fig. 5 for the measured reflectance spectra of aubrite (Norton County), carbonaceous chondrite (Allende), and enstatite chondrite (Abee).

apply the PCA formulation, discussed in Sec. 2.3, we receive 44 spectra in the new PCA basis. From the total variance in the data with 427 spectral variables, the three first PCA variables contain over 95 %, and the five first over 99 %. The three first PCA coordinate vectors (PCA vector for short) are shown in Fig. 10.

In Fig. 10, together with the PCA vectors, we plot the mean-corrected averaged spectra of the five meteorite types, namely the ordinary chondrites (OC), HED meteorites (HED), carbonaceous chondrites (CC), Aubrites, and enstatite chondrites (EC). The PCA value for variable i of the individual meteorite spectrum are formed by a dot product with the mean-centered spectrum and the PCA vector i. Therefore, the wavelengths with large (absolute) values (i.e., scores) in the PCA vector will have large weights in the corresponding PCA variable value.

The PCA vectors can be roughly summarized so that they take into account the spectral behavior around 0.9, 1.3, 2.1, and 2.5 µm wavelengths. How each of the three PCA vectors combine these wavelengths is shown in Table 3. The first vector gives negative weights for wavelengths around 0.9, 2.1, and 2.5 µm. Effectively, it will separate HED's with negative mean-corrected values at those wavelengths from EC with positive values. Note that the OC average mean-corrected spectra is approximately zero for all the wavelengths, so that it will be a neutral class in the PCA.

Table 3: PCA vectors summarized. Symbols '+' and '-' mean that the PCA vector will weight the wavelengths around the corresponding column title with large positive or negative values. No symbol means that the wavelengths have small weights.

PCA	wavelength (µm)			
vector	0.9	1.3	∼2.1	2.5
1	-		-	-
2		-	+	
3	+	-		-

The second PCA vector classifies according wavelengths around 1.3 and 2.1 µm. HEDs and CCs will be separated from Aubrites and ECs. The third PCA vector classifies according

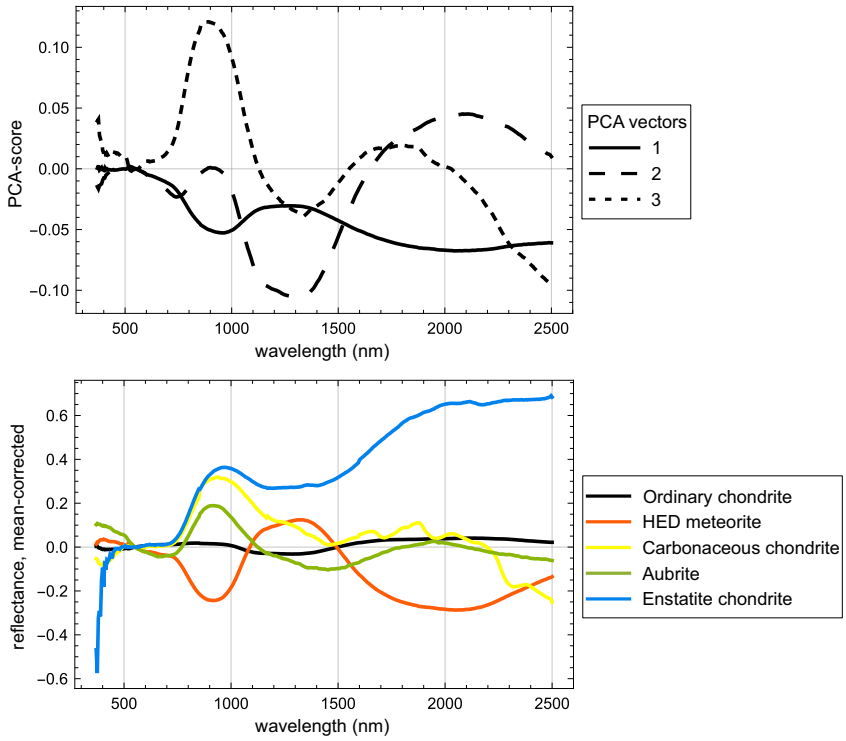

Figure 10: The three first PCA coordinate vectors are shown in the upper panel. In the lower panel, the mean-corrected averaged spectra of the five meteorite types are shown.

wavelengths around 0.9, 1.3, and 2.5 µm. HEDs and ECs will be separated from CCs and Aubrites. The resulting PCA variables for the individual meteorites are shown in Fig. 11.

The previous studies carried out by Paton et al. (2011)[20] and Pentikäinen et al. (2014)[21] suggest that HED meteorites can be separated from chondrites, and that ordinary chondrites can be grouped together. The results of the PCA computed here support these conclusions and show that also enstatites and aubrites can be separated. Separating carbonaceous chondrites from ordinary ones seems to be most challenging, but they do stand apart in the projection to the 2nd and 3rd PCA basis vectors.

We also tried to separate the H, L, and LL types of ordinary chondrites from each other using either the PCA analysis for all the meteorites, as described above, or by conducting the similar analysis only for the OCs. Hiroi et al. (2017)[22] reported a successful outcome on a PCA study for different types of carbonaceous chondrites, but we were not able to find consistent differences between the different OC types in our data (results not shown here).

The spectra of meteorites link them to their parent bodies, asteroids. Their spectral behavior is similar, but not directly the same. There are usually differences especially in the absolute reflectance level, on the strength of the absorption features, and on the spectral slope. These differences are due to their different surface characteristics. Asteroid observations are performed by studying scattering process in the fine, space-weathered regolith covering the bodies. Meteorite surfaces are free from regolith, have undergone some melt-

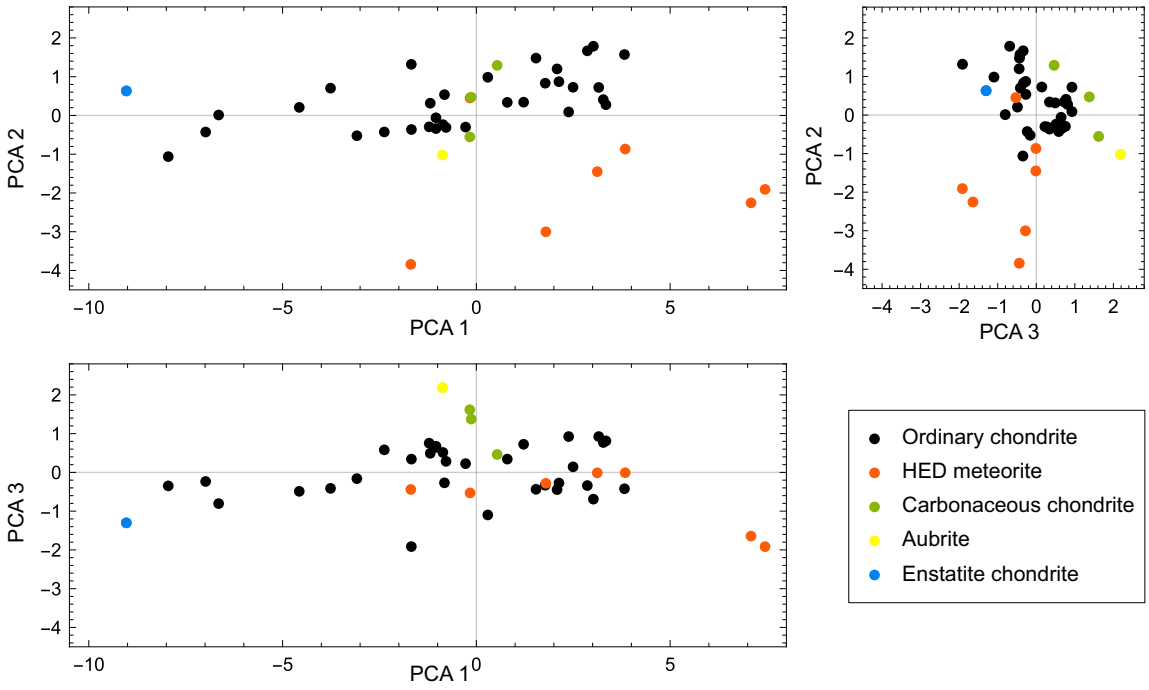

Figure 11: The spectra of 30 measured meteorites and 14 complementary meteorites from [17] presented in the coordinate basis of the three first PCA variables. The different panels in the figure give different orthogonal views to the three-dimensional data cloud along the PCA coordinate axis 1, 2, and 3.

ing, and probably more fresh (less space-weathered) than asteroid surface dust. However, tools such as the PCA can reveal their similarities and help us linking the counterparts in meteorites and asteroids more reliably.

Acknowledgements

We thank Arto Luttinen for granting us access to the mineral cabinet of the Geological Museum of the Finnish Museum of Natural History. The authors acknowledge the financial support from the European Research Council, Advanced Grant No. 320773 entitled Scattering and Absorption of Electromagnetic Waves in Particulate Media (SAEMPL).

References

[1] Bland, P.A., Smith, T.B., Jull, A.J.T., Berry, F.J., Bevan, A.W.R., Cloudt, S., Phillinger, C.T., The flux of meteorites to the earth over the last 50,000 years, Monthly Notices of the Royal Astronomical Society 283 (1996) 551–565.

[2] G. Drolshagen, D. Koschny, S. Drolshagen, J. Kretschmer, B. Poppe, Mass accumulation of earth from interplanetary dust, meteoroids, asteroids and comets, Planetary and Space Science 143 (Supplement C) (2017) 21–27. doi:10.1016/j.pss.2016.12.010.

[3] M. Gritsevich, V. Stulov, L. Turchak, Consequences of collisions of natural cosmic bodies with the Earth's atmosphere and surface, Cosmic Research 50 (1) (2012) 56–64. doi:10.1134/S0010952512010017.

[4] V. Dmitriev, V. Lupovka, M. Gritsevich, Orbit determination based on meteor observations using numerical integration of equations of motion, Planetary and Space Science 117 (Supplement C) (2015) 223–235. doi:10.1016/j.pss.2015.06.015.

[5] B. Gladman, J. Burns, The delivery of Martian and Lunar meteorites to Earth, Bulletin of the American Astronomical Society 28 (1996) 1054.

[6] Weisberg,M., McCoy,T., Krot,A., Systematics and evaluation of meteorite classification, in: D. Lauretta, H. McSween (Eds.), Meteorites and the Early Solar System II, University of Arizona Press, 2006, pp. 19–52.

[7] Bland, P., Zolensky, M., Benedix, G., Sephton, M., Weathering of chondritic meteorites, in: Lauretta, D.S., McSween, H.Y. Jr. (Eds.), Meteorites and the Early Solar System II, University of Arizona Press, 2006, pp. 853–867.

[8] Kohout, T., Gritsevich, M., Grokhovsky, V., Yakovlev, G., Haloda, J., Halodova, P., Michallik, R., Penttilä, A., Muinonen, K., Mineralogy, reflectance spectra, and physical properties of the Chelyabinsk LL5-chondrite — insight into shock induced changes in asteroid regoliths, Icarus 228 (2014) 78–85.

[9] D. Britt, C. Pieters, M. Petaev, N. Zaslavaskaya, The Tsarev meteorite — petrology and bidirectional reflectance spectra of a shock-blackened L chondrite, in: Proceedings of the 19th Lunar and Planetary Science Conference, Houston, Texas, USA, 1989, pp. 537–545.

[10] Sharp,T., De Carli,P., Shock effects in meteorites, in: Lauretta, D.S., McSween, H.Y. Jr. (Eds.), Meteorites and the Early Solar System II, University of Arizona Press, 2006, pp. 653–677.

[11] Chapman, C.R., Salisbury, J.W., Comparisons of meteorite and asteroid spectral reflectivities, Icarus 19 (1973) 507–522.

[12] M. Gaffey, Spectral reflectance characteristics of the meteorite classes, Journal of Geophysical Research 81 (1976) 905–920.

[13] M. Gaffey, T. McCord, Asteroid surface materials: Mineralogical characterisations from reflectance spectra, Space Science Reviews 21 (1978) 555–628.

[14] J. Martikainen, A. Penttilä, M. Gritsevich, H. Lindqvist, K. Muinonen, Spectral modeling of meteorites at UV-Vis-NIR wavelengths, Journal of Quantitative Spectroscopy and Radiative Transfer 204 (2018) 144–151. doi:10.1016/j.jqsrt.2017.09.017.

[15] M. Gaffey, E. Cloutis, M. Kelley, K. Reed, Mineralogy of asteroids, in: W. Bottke, A. Cellino, P. Paolicchi, R. Binzel (Eds.), Asteroids III, University of Arizona Press, 2002, pp. 183–204.

[16] J. Martikainen, Physical modeling for the Vis-SWIR spectrometry of the Chelyabinsk meteorite, Master's thesis, University of Helsinki, Finland (2016).
URL http://hdl.handle.net/10138/160874

[17] M. Gaffey, Meteorite spectra, EAR-A-3-RDR-METEORITE-SPECTRA-V2.0, NASA Planetary Data System (2001).

[18] R. Klima, C. Pieters, M. Dyar, Spectroscopy of synthetic Mg-Fe pyroxenes I: Spin-allowed and spin-forbidden crystal field bands in the visible and near-infrared, Meteoritics & Planetary Science 42 (2) (2007) 235–253. doi:10.1111/j.1945-5100.2007.tb00230.x.

[19] M. Taran, S. Matsyuk, Fe2+, Mg-distribution among non-equivalent structural sites M1 and M2 in natural olivines: an optical spectroscopy study, Physics and Chemistry of Minerals 40 (4) (2013) 309–318. doi:10.1007/s00269-013-0572-x.

[20] Paton, M., Muinonen, K., Pesonen, L., Kuosmanen, V., Kohout, T., Laitinen J., Lehtinen, M., A PCA study to determine how features in meteorite reflectance spectra vary with the samples' physical properties, Journal of Quantitative Spectroscopy and Radiative Transfer 112 (2011) 1803–1814.

[21] Pentikäinen, H., Penttilä, A., Muinonen, K., Peltoniemi, J., Spectroscopic investigations of meteorites, Journal of Quantitative Spectroscopy and Radiative Transfer 146 (2014) 391–401.

[22] T. Hiroi, R. Milliken, C. Pieters, H. Kaiden, N. Imae, A. Yamaguchi, H. Kojima, S. Sasaki, M. Matsuoka, Y. Sato, T. Nakamura, Visible and near-infrared spectral survey of carbonaceous chondrites and its application to Hayabusa2, in: Proceedings of the 48th Lunar and Planetary Science Conference, The Woodlands, Texas, USA, 2017, p. 1086.